Use of non-natural amino acids for the design and synthesis of a selective, cell-permeable MALT1 activity-based probe

Merel A. T. van de Plassche,[1] Thomas J. O'Neill,[2] Thomas Seeholzer,[2] Boris Turk,[3] Daniel Krappmann,[2] and Steven H. L. Verhelst[*, 1,4]

[1] KU Leuven, Department of Cellular and Molecular Medicine, Laboratory of Chemical Biology, Herestr. 49, 3000 Leuven, Belgium
[2] Research Unit Cellular Signal Integration, Institute of Molecular Toxicology and Pharmacology, Helmholtz Zentrum München, Ingolstaedter Landstrasse 1, 85764, Neuherberg, Germany
[3] Department of Biochemistry and Molecular and Structural Biology, J. Stefan Institute, Jamova 39, Sl-1000 Ljubljana, Slovenia
[4] Leibniz Institute for Analytical Sciences ISAS, e.V., Otto-Hahn-Str. 6b, 44227 Dortmund, Germany

ABSTRACT: Constitutive proteolytic activity of MALT1 is associated with highly aggressive B cell lymphomas. Chemical tools that detect active MALT1 have been reported, but suffer from poor cell-permeability and/or cross-reactivity with the cysteine protease cathepsin B. We here report that the non-natural amino acid pipecolinic acid in the P2 position of substrates and chemical probes leads to improved selectivity towards MALT1 and results in cell permeable fluorescent probes.

INTRODUCTION

MALT1 (mucosa-associated lymphoid tissue lymphoma translocation protein 1) is the only human paracaspase: a cysteine protease that belongs to the caspase family, but displays a preference for arginine in the P1 position instead of aspartic acid (Figure 1A). It is part of the CARMA1-BCL10-MALT1 (CBM) complex, which controls various aspects of signal transmissions essential for nuclear factor κB (NF-κB) and Jun N-terminal kinase (JNK) activation upon antigenic stimulation in T and B lymphocytes.[1,2] MALT1 regulates lymphocyte activation in two different ways: as a scaffolding protein in the CBM complex, and as a protease. Whereas the MALT1 scaffolding function is essential for canonical NF-κB and JNK activation, MALT1 proteolytic activity modulates lymphocyte activation by cleaving distinct substrates that are involved in signaling (e.g. TNFAIP3/A20, CYLD and HOIL1) as well as transcriptional (e.g. RelB) or post-transcriptional (Regnase-1, Roquin1/2) gene regulation.[3,4] MALT1 has received considerable biomedical attention, because constitutive protease activity has been found in highly aggressive diffuse large B cell lymphoma (DLBCL), the most common type of non-Hodgkin lymphoma (NHL). Both active site[5] and allosteric inhibitors[6,7] of MALT1 show suppression of B-cell lymphoma tumor growth *in vitro* and *in vivo*. Based on these preclinical data, the first clinical trial evaluating the therapeutic potential of MALT1 inhibitors in NHL and chronic lymphocytic leukemia has been initiated (NCT03900598). Additionally, MALT1 paracaspase-deficiency as well as allosteric MALT1 inhibitors protect mice from experimental autoimmune encephalomyelitis, a model used to study autoimmune and inflammatory reactions associated with humans, such as Multiple Sclerosis (MS).[8,9] Despite the pathophysiological relevance of MALT1 protease activity, selective small molecule tools such as activity-based probes (ABPs) that can be used in whole cells, are still missing.[10,11] These would enable detection of active MALT1 in clinical samples, allowing stratification of patients and measurement of on-target activity during treatment. Furthermore, MALT1 ABPs could be used to further study the role of MALT1 in MS and DLBCL in cellular and animal models.

Based on the covalent tetrapeptide MALT1 paracaspase inhibitor Z-VRPR-FMK,[12] two research groups independently developed the first MALT1 ABPs.[13,14] These probes label active MALT1 in cell lysates and whole cells, but suffer from cross-reactivity with the lysosomal cysteine protease cathepsin B (CatB), which also prefers an arginine residue in the P1 position.[15] Although specific detection of active MALT1 was achieved using one of these ABPs in combination with a MALT1 antibody in an enzyme-linked activity-sorbent assay,[13] more selective probes are required for selective detection of active MALT1 in bulk or single cell assays. In order to overcome cross-reactivity with CatB, we explored the use of non-natural amino acids. We chose the approach of a hybrid combinatorial substrate library (HyCoSuL) to screen for non-natural amino acid preferences of the different protease recognition pockets.[16] Specifically, HyCoSuL creates fluorogenic substrates with different non-natural amino acids in the P2, P3 or P4 position, re-

spectively, and mixed natural amino acids in the other positions (Figure 1B). The most promising substrate sequences are then used as recognition elements for MALT1 ABPs (Figure 1C).

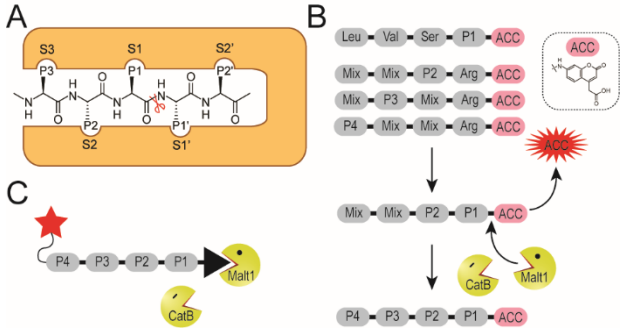

Figure 1. A schematic overview of the general approach for the design of selective ABPs for MALT1 (A) Summary of the Schechter and Berger nomenclature of protease substrates.[17] The P1, P2, P3 etc. positions correspond to the amino acids at the N-terminal side of the scissile bond of the substrate. S1, S2 etc. corresponds to the respective pockets of the protease. Similar residues and pockets towards the C-terminus of the substrate are designated by an apostrophe (P1', S1' etc.). (B) Schematic representation of a positional scanning library. Our particular HyCoSuL consists of three (ACC)-labeled sublibraries (P2, P3 and P4) that are synthesized on solid phase. They contain a fixed P1 Arg, different non-natural amino acids in each member of the P2, P3 or P4 sublibrary, and in the other positions a mixture of 19 natural amino acids (the 20 proteinogenic amino acids minus Cys and Met, and with norleucine as a methionine analog). Next, these sublibraries are screened for MALT1 and CatB to find amino acids in the P2, P3 and P4 position that are recognized by MALT1, but not by CatB. The most active and selective amino acids are then used for the synthesis of individual 7-Amino-4-carbamoylmethylcoumarin (ACC)-labeled substrates. (C) The optimal sequence found in the HyCoSuL is used as a basis for the design of a new ABP. An ABP generally contains an electrophilic warhead (triangle), which reacts with the active site of the target protease, a recognition element to increase affinity and selectivity, and a detection tag (star) for analysis of the probe-protease complex.

RESULTS AND DISCUSSION

An initial screen for different arginine analogs in the P1 position revealed that the natural amino acid arginine was by far the best recognition element for MALT1 (Figure S1). Consequently, we decided to synthesize the HyCoSuL with an arginine in the P1 position. A previously reported positional library scan with natural amino acids found that MALT1 only accepts small amino acids in the P2 position, including proline, whereas it exhibits a greater tolerance for the P3 position with a preference for valine and other non-polar amino acids, and favors leucine in the P4 position.[18] Based on this knowledge, we chose a number of non-natural amino acids (structures in Figure S2) that could fit in the S2, S3 and S4 pockets for the generation of a small, focused HyCoSuL. The library was synthesized by solid phase peptide synthesis as described by Drag and coworkers.[16] A slight adjustment was made for couplings to amino acids with a secondary amine or α-,α-di-substituted amino acids, as we noticed that these reactions did not go to completion using HOBt/DIC. Hence, HATU and DIEA were used as coupling reagents, resulting in complete coupling to the resin-bound intermediate.

We tested the synthesized library against both MALT1 and CatB by measuring the increase in fluorescence over time in a fluorescence platereader. We found that MALT1 tolerates both serine and proline homologues in the P2 position (Figure 2). Whereas library members with some non-natural amino acids exerted detrimental effects to both enzymes (e.g. **SL-5**, **SL-9**), a number of library members with other non-natural amino acids strongly increased the preference for CatB processing over MALT1 (e.g. **SL-4**, **SL-15**), which is the opposite of our objective. Interestingly, the library member with the proline analog L-pipecolinic acid (Pip, **SL-3**) in the P2 position showed significantly slower processing by CatB and slightly faster processing by MALT1 compared with the natural P2 Ser library member. In an earlier reported positional library scan with non-natural amino acids for MALT1, Pip was not found as a hit.[19] This may be attributed to an incomplete peptide-coupling step in the synthesis under the utilized DIC/HOBt coupling conditions and the inability of the standard Kaiser test to detect residual secondary amines (Figure S3). In the P3 position, both CatB and MALT1 tolerated a wide variety of amino acids, but none showed significantly faster processing by MALT1 compared with CatB. In the P4 position, we found that the library member with the cyclic amino acid AC6C (**SL-23**) was processed faster by MALT1 and slower by CatB compared with the P4 Leu library member (Figure 2).

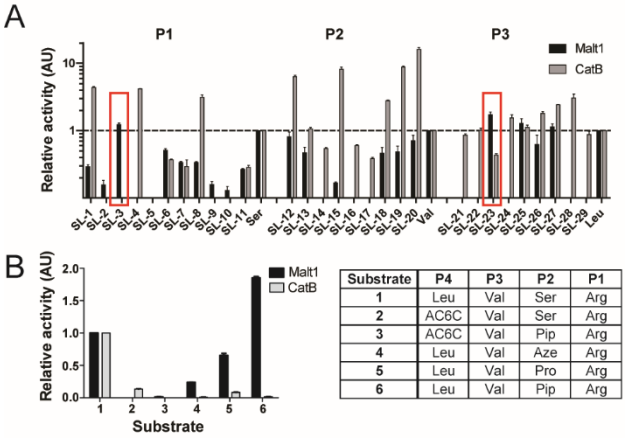

Substrate	P4	P3	P2	P1
1	Leu	Val	Ser	Arg
2	AC6C	Val	Ser	Arg
3	AC6C	Val	Pip	Arg
4	Leu	Val	Aze	Arg
5	Leu	Val	Pro	Arg
6	Leu	Val	Pip	Arg

Figure 2. (A) An overview of the relative activity of each synthesized library member for MALT1 and CatB, where Pip (SL-3) and AC6C (SL-23) are found as initial hits. Values shown represent the slope of the linear part of the measured curve, normalized against the slope of the optimal natural amino acid in that respective position. Data shown is the average of three independent experiments. (B) The relative activity of new substrates **1-6** for MALT1 and CatB.

To validate promising hits from the HyCoSuL, we selected the P2 Pip and P4 AC6C to synthesize individual substrates **2**, **3** and **6**. Since MALT1 seems to tolerate a ring structure in the P2 position, we also included azetidine-2-carboxylic acid (Aze) and proline in the P2 position, which were not included in our original HyCoSuL (substrates **4**

and **5**, respectively). All newly synthesized substrates were compared with the previously found optimal substrate LVSR-ACC.[18] Screening of the resulting six individual substrates against MALT1 and CatB showed that the substrate with Pip in the P2 showed the fastest processing by MALT1 (Figure 2B, full structures in Figure S4). Proline and azetidine were both tolerated in the P2 position, but were cleaved more slowly compared with Pip. All three ring structures in P2 were poorly tolerated by CatB. The non-natural AC6C in P4, although found as a hit in the library scan, resulted in little to no proteolytic processing by MALT1. This false positive result in the library scan may be explained by subsite cooperativity with other amino acids in the P2 and P3 position, especially considering that AC6C is a sterically strained amino acid that may impose a distinct conformation on the peptide substrate. Hence, these sequences were not selected for further ABP development.

Scheme 1: The general synthesis route of the new ABPs.[a]

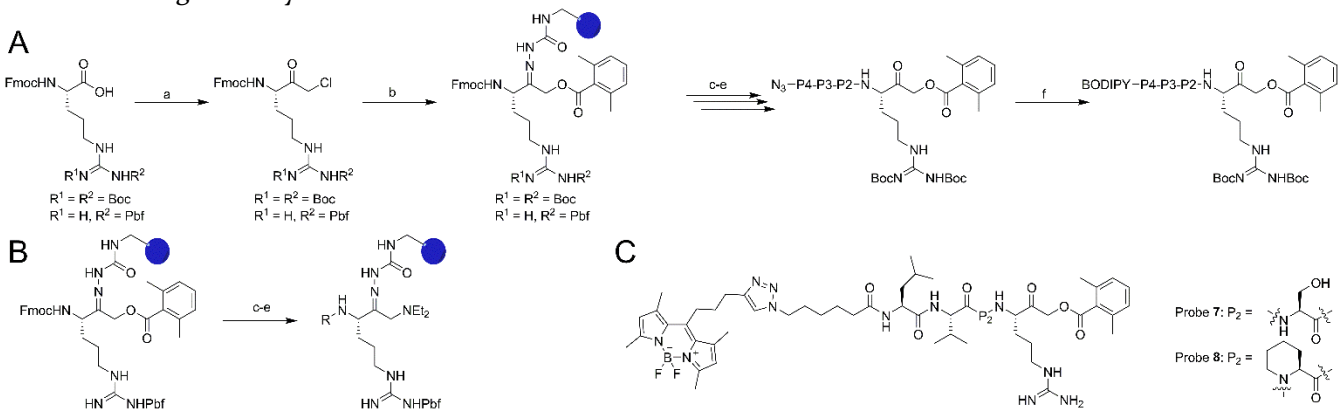

[a] Reagents and conditions: (a) (i) Isobutyl chloroformate, N-methylmorpholine, diazomethane, THF (ii) HCl/AcOH (b) dimethyl benzoic acid, KF, DMF (c) 5% DEA in DMF (d) Fmoc-AA-OH, HOBt, DIC/HATU, DIEA, DMF (e) 95% TFA/H_2O (d) DIEA, CuBr, BODIPY-alkyne, DCM.

LVPipR, the most selective substrate sequence, was used as a basis to synthesize a MALT1 ABP. As a warhead we chose the acyloxymethylketone (AOMK) electrophile, which is specific for cysteine proteases, compatible with solid phase peptide synthesis,[20] and has been used in all previous MALT1 probes.[13,14,19]

During elongation of the 2,2,4,6,7-pentamethyldihydrobenzofuran-5-sulfonyl (Pbf) protected arginine AOMK, attached to a solid phase resin through a hydrazone linkage, we noticed that the reported Fmoc deprotection conditions (5% diethylamine or 0.1 M tetrabutylammonium fluoride in DMF) were not compatible with the AOMK group. We hypothesized that the free guanidine NH group of the Pbf-protected arginine side chain may affect the stability of the AOMK under basic conditions (Scheme 1B). Indeed, a di-Boc-protected arginine AOMK was stable under the basic Fmoc deprotection conditions. After elongation with the amino acids for the P2, P3 and P4 position, and capping of the N-terminus with 6-azido-hexanoic acid, the probe was cleaved from the resin and coupled to an alkyne-functionalized boron-dipyrromethene (BODIPY) fluorophore[21] using copper catalyzed click chemistry to yield fluorescence coupled probes **7-8** (Scheme 1A and 1C).

To verify the increase in selectivity of the probes towards MALT1, we performed inhibition assays on purified MALT1 and CatB to compare our newly designed probes to a previously published ABP (MALT1-probe **9**, Figure S5)[13] and the commercially available active site inhibitor Z-VRPR-FMK.[13,14] All four compounds showed a comparable inhibition for MALT1, with the Z-VRPR-FMK showing slightly higher potency than the AOMK based probes, likely due to the higher electrophilicity of the FMK warhead. While the compounds containing natural amino acids (**7**, **9** and Z-VRPR-FMK) displayed similar potency in MALT1 and CatB inhibition, the unnatural amino acid in the new probe **8** rendered the probe substantially (~50-fold) less reactive towards CatB, demonstrating that the P2 Pip drastically improves the probe selectivity for MALT1 (Figure 3A). To further characterize the potency of probes **7-9**, we determined the K_i and k_{inact} for each. K_i represents the binding constant between the protease and the probe, while k_{inact} reflects the rate of covalent bond formation. In line with previous results, all three probes show similar K_i and k_{inact} values for MALT1. Strikingly, new probe **8** displays a substantial increase in K_i for CatB, confirming that the unnatural Pip in the P2 position decreases the affinity of the probe for CatB (Figure 3B).

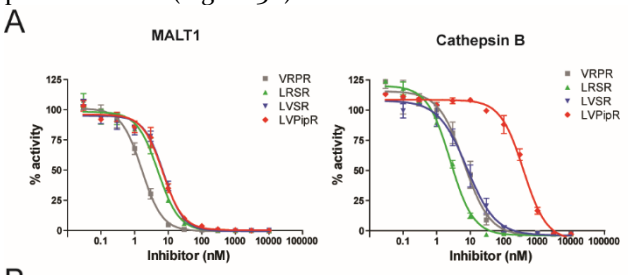

B

	K_i (μM) MALT1	K_{inact} (10^{-3} s^{-1}) MALT1	K_i (μM) CatB	K_{inact} (10^{-3} s^{-1}) CatB
Probe **7**	0.21 ± 0.04	1.1 ± 0.1	0.21 ± 0.06	4.1 ± 0.30
Probe **8**	0.17 ± 0.02	1.7 ± 0.07	>10	N.D.
Probe **9**	0.34 ± 0.08	2.0 ± 0.2	0.63 ± 0.14	9.6 ± 0.9

Figure 3. initial charaterization of MALT1 probes. (A) Activity of probes **7-9** and inhibitor Z-VRPR-FMK against MALT1 and CatB, measured in a fluorescent plate reader assay. Data shown is the average of three independent experiments. (B) Kinetic parameters K_i and k_{inact} of probe **7-9** for MALT1 and CatB. N.D.: value could not be determined. Curves of K_i and k_{inact} are provided in Figure S6.

To gain insight into the binding mode of probe **8**, we performed covalent docking of the MALT1-probe **8** complex

using the flexible side chain method of Autodock 4.2.[22] The pose with the lowest binding energy clearly shows the importance of the P1 residue: the arginine side chain reaches deep into the S1 pocket, where the guanidine group forms interactions with the negatively charged side chains of D462, D365 and E500 (Figure 4). Comparison with the crystal structure of the previously reported LRSR-AOMK probe in complex with MALT1[13] reveals that switching the P2 position from serine to Pip causes the loss of one hydrogen bond between the serine side chain and MALT1 (Figure 4, Figure S7). The probe-protease interactions in the P3 and P4 pockets appear to be mostly hydrophobic interactions, explaining the preference of MALT1 for hydrophobic amino acids in these positions. Overall, the LVPipR sequence displays a good overlay with crystal structures of the LRSR probe (Figure 4), explaining the comparable affinity for MALT1.

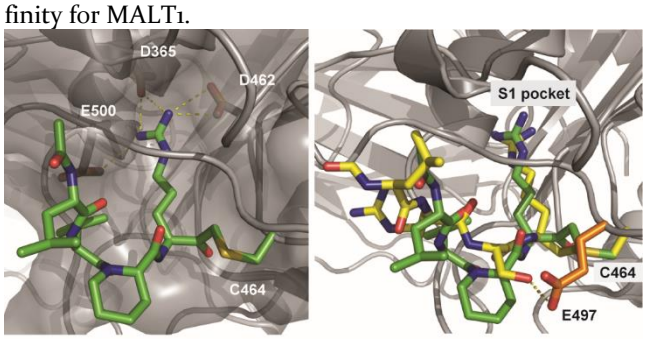

Figure 4. Left panel: A close-up view of the MALT1 active site (PDB code: 4I1P), with a docked structure of covalently bound probe **8**. The enzyme is depicted in cartoon mode and partially as transparent surface representation. Probe **8** is depicted as stick model. Right panel: overlay of the docked structure of probe **8** (in green stick model) with the crystal structure of probe **9** (in yellow stick model), covalently bound to MALT1.

Next, we tested the ability of the new probes to covalently label active MALT1. For recombinant MALT1 high chaotropic salt concentrations are required to activate protease activity, which complicates *in vitro* analysis of probe efficiency. Thus, we worked with MALT1 KO Jurkat T-cells stably reconstituted with StrepTagII-tagged MALT1B wild type or the catalytically inactive MALT1B catalytic site mutant (C453/A).[23] This allows for specific isolation and enrichment of MALT1 after activation, enabling analysis even with very low abundance of active MALT1. All three BODIPY probes (**7**, **8** and **9**) clearly label active MALT1B only after T cell stimulation using P/I (phorbol 12-myristate 13-acetate/ionomycin) stimulation. Activity was confirmed by cleavage of the endogenous subtrate CYLD. No labeling and activity was observed for the MALT1B C/A catalytic site mutant, confirming that the probes form a covalent bond with the active site cysteine (Figure 5A).

After confirming labeling of MALT1 by the new probe **8**, we assessed whether it shows improved selectivity. To this end, whole cell lysates of wild type Jurkat T-cells were incubated with probes **7**, **8** or **9**. As expected, covalent complexes of endogenous MALT1 and the ABPs were only detected after P/I stimulation. Gratifyingly, probe **8** did not show any CatB signal, whereas the other probes clearly displayed CatB labeling independent of stimulation (Figure 5B). As expected, while formation of the MALT1-probe **7** complex was inhibited by MALT1 inhibitor S-Mepazine and Z-VRPR-FMK, the CatB-probe **7** adduct was abolished by the cross-reacting Z-VRPR-FMK as well as the CatB-specific C4074Me inhibitor (Figure 5C), confirming the identity of the detected proteins.

Besides cross-reactivity with CatB, previous experiments have shown that the existing MALT1 ABPs suffered from poor target engagement in living cells, which is most likely due to inefficient cellular uptake. Thus, we treated the human B-cell lymphoma cell line HBL1, which displays chronic MALT1 protease activity[13] with probes **7**, **8** or **9** for 5 hours and determined cellular MALT1 inhibition by detecting RelB substrate cleavage (Figure 5D). While probe **9** is not inhibiting cellular MALT1 activity, probe **7** and **8** are inhibiting RelB cleavage in a dose dependent manner, demonstrating that they reach the target in intact cells.

Additionally, we treated stimulated and unstimulated Jurkat T-cells with the different probes for 3 hours. This experiment confirmed poor target engagement of probe **9**, which only shows faint labeling of both MALT1 and CatB when administered to living cells, suggesting that it does not enter the cell properly (Figure 5E). Probe **7** shows stronger labeling of MALT1, but also strong labeling of CatB – even stronger than in lysates. This may be explained by cellular uptake of the probes via endocytosis, which leads to an efficient transport to the site of active CatB in the lysosomes before the probes encounter MALT1 in the cytosol. Additionally, the buffer used in the experiments on cell lysates does not have the optimal pH for CatB activity, which likely contributes to the lower signal in cell lysates. Importantly, probe **8** did not show any detectable CatB labeling, but strong MALT1 labeling, proving not only a strong improvement in selectivity over probe **7** and **9**, but also efficient labeling in cells compared with probe **9** (Figure 5E).

CONCLUSION

In conclusion, we designed a new and selective ABP targeting MALT1 based on HyCoSuL screening using unnatural amino acids. The novel probe is able to distinguish between active and inactive MALT1 protease and displays an improved cell permeability compared with its predecessors. Importantly, non-natural pipecolinic acid in the P2 position severely decreased cross-reactivity with CatB *in vitro*, preventing CatB cross-labeling in cells. We expect that this new probe with increased MALT1 selectivity and cell permeability represents a further step in the design and synthesis of a MALT1 ABP that can be used for MALT1 detection at the single cell level.

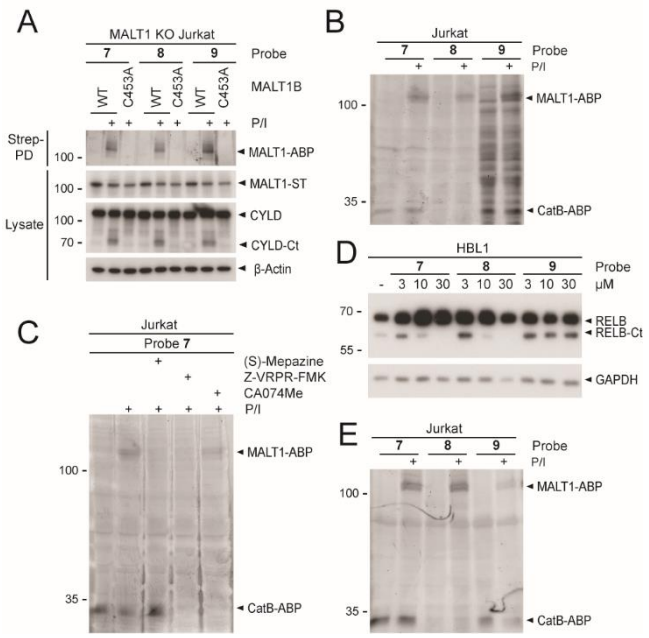

Figure 5. A direct comparison of probes **7-9** in cell lysates and living cells reveals highly selective labeling by probe **8**. (A) ABP labeling of MALT1 after pulldown from Jurkat T-cell lysates. MALT1 is only labeled after P/I stimulation of the cells, which activates the NF-κB pathway. The probes do not label the catalytic mutant MALT1-C453A. Expression and activity of MALT1B wt and C453A is confirmed by Western Blot. (B) Labeling of the lysate of stimulated and unstimulated Jurkat T-cells with probe **7**, **8** or **9**. (C) Competition between probe labeling and various inhibitors: allosteric MALT1 selective inhibitor (S)-mepazine, promiscuous inhibitor Z-VRPR-FMK and cathepsin B inhibitor CA-074Me. Migration of MALT1- and CatB-ABP complexes is indicated. (D) Dose dependent effects on cellular MALT1 activity by probe **7**, **8** and **9** were determined by inhibition of RelB substrate cleavage. (E) Whole cell labeling of stimulated and unstimulated Jurkat T-cells with probe **7**, **8** or **9**.

EXPERIMENTAL SECTION

General chemistry. All starting materials and solvents were bought from commercial vendors and used without further purification. Reactions were analyzed by Thin Layer Chromatography (TLC) on pre coated 0.20 mm thick ALUGRAM® TLC sheets with fluorescent indicator and by liquid chromatography-mass spectrometry (LC-MS) performed on a Prominence Ultra-fast Liquid Chromatography system equipped with a 2x150 mm C18 analytical column (Waters X-Bridge) coupled to a MS-2020 single quadrupole mass analyzer (Shimadzu). HRMS spectra were acquired on a quadrupole orthogonal acceleration time-of-flight mass spectrometer (Gynapt G2 HDMS, Waters, Milford, MA). Silica column chromatography was performed using 230-400 mesh silica (Kieselgel 60). High Pressure Liquid Chromatography (HPLC) purification was performed using a 10x150 mm C18 preparative column (X-Bridge). A linear gradient of 20-80% acetonitrile in water (with 0.1% TFA) was utilized. The purity of all final compounds tested was determined to be ≥95% using liquid chromatography-mass spectrometry (LC-MS).

7-Amino-4-carbamoylmethylcoumarin (ACC) synthesis. ACC building block was synthesized as described by Maly et al.[24]

General synthesis of substrate libraries. The HyCoSuL was synthesized as described by Drag et al.[16] For amino acids with a secondary amine or α-,α-di-substituted amino acids (3 eq.), HATU (3 eq.) and DIEA (3 eq.) were used as coupling reagents instead of HOBt/DIC. Completion of these couplings was tested using a chloranil test instead of a Kaiser test.

General synthesis of individual substrates. Individual substrates **1-6** were synthesized as described by Drag et al.[16] The resin loading was estimated by UV absorption of free Fmoc and used for calculation of the yield. For amino acids with a secondary amine or α-,α-di-substituted amino acids (3 eq.), HATU (3 eq.) and DIEA (3 eq.) were used as coupling reagents instead of HOBt/DIC. Completion of these couplings was tested using a chloranil test instead of a Kaiser test. All substrates were purified by reversed-phase HPLC. Fractions containing product were pooled and lyophilized.

Substrate 1 (Ac-L-V-S-R-ACC). 10.7% yield. HRMS (MALDI-TOF): m/z calculated for $C_{33}H_{49}N_9O_9$ [M+H]+ 716.3725, found 716.3737.

Substrate 2 (Ac-AC6C-V-S-R-ACC). 18.3% yield. HRMS (MALDI-TOF): m/z calculated for $C_{34}H_{49}N_9O_9$ [M+H]+ 728.3725, found 728.3730.

Substrate 3 (Ac-AC6C-V-Pip-R-ACC). 19.0% yield. HRMS (MALDI-TOF): m/z calculated for $C_{37}H_{53}N_9O_8$ [M+H]+ 752.4089, found 752.4097.

Substrate 4 (Ac-L-V-Aze-R-ACC). 4.6% yield. HRMS (MALDI-TOF): m/z calculated for $C_{34}H_{49}N_9O_8$ [M+H]+ 712.3776, found 712.3768.

Substrate 5 (Ac-L-V-P-R-ACC). 15.3% yield. HRMS (MALDI-TOF): m/z calculated for $C_{35}H_{51}N_9O_8$ [M+H]+ 726.3933, found 726.3934.

Substrate 6 (Ac-L-V-Pip-R-ACC). 9.8% yield. HRMS (MALDI-TOF): m/z calculated for $C_{36}H_{53}N_9O_8$ [M+H]+ 740.4089, found 740.4076.

Library screen. The library screen was performed on a SpectraMax iD3 Multi-Mode Microplate Reader (Molecular Devices) using 96-well black plates with 355 nm excitation and 460 nm emission. The total substrate library concentration used was 50 μM per well, diluted from a 5 mM stock in DMSO (1% final DMSO concentration) in MALT1 activity buffer (50 mM HEPES pH 7.5, 0.9 M ammonium citrate, 100 mM NaCl, 1 mM EDTA and 10 mM DTT (added directly before use)). 0.2 μM of N-terminally GST-tagged MALT1 catalytic domain (amino acids 325–760), expressed as previously described[18], was preactivated in MALT1 activity buffer for 20 min at 37 °C before adding to the library (0.1 μM final MALT1 concentration). Fluorescence intensity was determined over the course of 2 hours at 37 °C for MALT1. For CatB, expressed as previously described[25], 2 nM of protein in acetate buffer (50 mM sodium acetate pH 5.5, 5 mM MgCl and 1 mM DTT (added directly before use)) was measured for 30 min at room temperature. Every library was measured in triplicate, and a blank without pro-

tease was measured and subtracted from the measurements. The values obtained for each substrate were plotted in excel to calculate the linear part of the slope in RFU/s. These values were normalized to the average value obtained for the best natural amino acid in that position (highest production of relative fluorescence units per second), and plotted in a bar graph. SEM values were calculated in GraphPad Prism.

Fmoc-Arg(Boc)$_2$-CMK. *N*-alpha-(9-Fluorenylmethyloxycarbonyl)-N',N''-bis-*t*-butyloxycarbonyl-L-arginine (Fmoc-Arg(Boc)$_2$-OH) was converted into a chloromethyl ketone (CMK) using a previously described synthetic procedure.[20] The product was purified using column chromatography (petroleum ether : ethyl acetate, 4:1). Fmoc-Arg(Boc)$_2$-CMK was obtained as a yellow oil (84% crude yield) and was used for the next reaction.
LC-MS: m/z calculated for $C_{32}H_{41}ClN_4O_7$ [M+H] 629.27, found 629.05. ^{1}H NMR (300 MHz, $CDCl_3$): δ 11.50 (s, 1H), 8.43 (s, 1H), δ 7.76 (d, *J* = 7.5 Hz, 2H), 7.62 (dd, *J* = 12.4, 7.6 Hz, 2H), 7.40 (t, *J* = 7.4 Hz, 2H), 7.31 (dd, *J* = 9.3, 5.3 Hz, 2H), 6.29 (d, *J* = 7.8 Hz, 1H), 4.55 (s, 1H), 4.46 (d, *J* = 6.8 Hz, 1H), 4.31 (d, *J* = 4.0 Hz, 1H), 4.21 (t, *J* = 6.6 Hz, 1H), 3.46 (d, *J* = 45.2 Hz, 2H), 2.02 (d, *J* = 8.1 Hz, 1H), 1.82 (d, *J* = 34.6 Hz, 2H), 1.77 – 1.52 (m, 3H), 1.54 – 1.41 (m, 18H), 1.31 – 1.20 (m, 1H).

Azido-hexanoyl-peptidyl-AOMKs. A 0.5 M solution of 3 eq Fmoc-Arg(Boc)$_2$-CMK was added to the resin in a solid phase cartridge and gently shaken at 50 ºC for 3 hours. After incubation, the solution was removed and resin was washed 3 times with DMF. 5 eq of 2,6-dimethylbenzoic acid and 10 eq potassium fluoride in DMF were added and the reaction mixture was gently shaken overnight at room temperature. The solution was removed and the resin was washed 3 times with methanol, DMF and DCM, and dried. The resin loading was estimated by UV absorption of free Fmoc at 290 nm.

The N-terminal Fmoc group was removed by incubating the resin with 5% diethylamine (DEA) in DMF for 2 times 15 min. The resin was washed 3 times with DMF and DCM. 3 eq *N*-Fmoc-protected amino acid and 3 eq of HOBt/DIC were dissolved in DMF (0.2 M final concentration) and added to the resin. The resin was shaken at room temperature for 3 hours, and washed 3 times with DMF and DCM. For each subsequent step of the solid phase peptide synthesis, the same deprotection and coupling reactions were used. However, when an amino acid was coupled to the free amine group of pipecolinic acid, the Fmoc amino acid (3 eq) was preactivated with 3 eq of HATU/DIPEA for 2 min, added to the resin and gently shaken for 3h at room temperature. Coupling reactions were monitored by the Kaiser test for primary amines, and a chloranil test for secondary amines. The peptide was capped with 6-azidohexanoic acid, which was synthesized according to a previously described procedure.[26] The product was cleaved off the resin with a TFA/TIPS/H_2O mixture (v/v/v, 95:2.5:2.5) and the solvent was removed under pressure. The final product was purified by reversed-phase HPLC. Fractions containing product were pooled and lyophilized.

Click chemistry. The respective AOMK peptide was dissolved in DCM and 1 eq of CuBr and 3 eq of DIPEA were added. Lastly, 1.05 eq of 5,5-difluoro-1,3,7,9-tetramethyl-10-(pent-4-yn-1-yl)-5H-4λ 4 ,5λ 4 -dipyrrolo[1,2-c:2',1'-f][1,3,2]diazaborinine, synthesized via a previously published procedure, was added.[21] Reaction mixture was stirred for 1 hour at room temperature. The solvent was removed under pressure and the final probe was purified by reversed-phase HPLC. Fractions containing product were pooled and lyophilized.

Probe 7 (BODIPY-Ahx-Leu-Val-Ser-Arg-AOMK). 18.7% yield. HRMS (MALDI-TOF): m/z calculated for $C_{55}H_{80}BF_2N_{11}O_8$ [M+H]+ 1073.6277, found 1073.6279.

Probe 8 (BODIPY-Ahx-Leu-Val-Pip-Arg-AOMK). 23.6% yield. HRMS (MALDI-TOF): m/z calculated for $C_{57}H_{83}BF_2N_{12}O_7$ [M+H]+ 1097.6641, found 1097.6650.

Inhibition assay. N-terminal GST-tagged Malt1 325-760 was diluted in Malt1 activity buffer (50 mM MES, pH 7.0, 150 mMNaCl, 10% Saccharose (w/v), 0.1% CHAPS (w/v), 1 M trisodium citrate, 10 mM DTT) to a concentration of 25 ng/18.5 µL in each well of a black, flat-bottom, 384-well microplate (Greiner Bio-One). 0.5 µL of inhibitor diluted in DMSO was added to the desired final concentration and incubated for 20 min at room temperature followed by the addition of 1 µL of Ac-LRSR-AMC substrate (Peptides International) at a final concentration of 50 µM. For CatB, 50 pg of protein was used in acetate buffer and 50 µM of the CatB substrate zRR-AMC. Fluorescence was measured in a Biotek Synergy 2 multi-detection microplate reader at 360 nm excitation and 460 nm emission for 3 hours at 30 °C. All experiments were performed in duplicate. For quantification, linear segments of cleavage activity were taken from 60-120 min for Malt1 and 60-80 min for CatB and compared to DMSO-treated controls.

Kinetic evaluation. Different probe concentrations diluted in DMSO were mixed together with 400 µM Ac-LVPipR-ACC substrate in MALT1 activity buffer (50 mM HEPES pH 7.5, 0.9 M ammonium citrate, 100 mM NaCl, 1 mM EDTA and 10 mM DTT (added directly before use)). 50 µL was added to each well of a black, flat-bottom, 96-well plate. N-terminal GST-tagged Malt1 325-760 was diluted in Malt1 cleavage buffer MALT1 activity buffer to a final concentration of 0,2 uM and 50 µL of protease was added to each well and fluorescence was measured for two hours at 355 nm excitation and 460 nm emission in a SpectraMax iD3 Multi-Mode Microplate Reader (Molecular Devices). For CatB, 0,4 nM of protein was used in acetate buffer and 400 µM of the CatB substrate zRR-AMC. Every measurement was done in triplicate, and a blank without protease was measured and subtracted from the measurements. For quantification, linear parts of the curve were taken and fitted into the equation $[P] = \frac{v_i}{k_{obs}}[1 - e^{-k_{obs}t}]$ to derive k_{obs}. k_{obs} was plotted against inhibitor concentration and the curves were fitted into the equation $k_{obs} = \frac{k_{inact}}{1+\frac{K_I}{[I]}}$ to derive the K_I and k_{inact} for each probe.

Covalent docking. Probe 8 was attached to the side chain of residue CYS 464 of MALT1 (PDB: 4l1P) and docked according to the flexible side chain method.[22] The probe 8 input file was drawn in Chemdraw professional 15.1, converted to a pdb file using Chem3D 15.1 and converted into

a PDBQT by autodocktools 1.5.6. The connected complex was treated as a fully flexible side chain. The binding site was covered by preparing a 40 × 48 × 40 size grid box with grid spacing of 0.375 Å and the center at 28.6222, 36.995, 9.772.

MALT1-ABP Labeling after MALT1 pull-down. Jurkat T-cells (MALT1B-StrepTagII and MALT1B C453A-StrepTagII)[23] were grown in standard RPMI medium containing 10% FCS (fetal calf serum), 100 U/mL penicillin/streptomycin and 2 mM glutamine. Jurkat T-cells were centrifuged at 350 x g for 5 min, resuspended in RPMI at a concentration of 1.5x10^7 cells/mL, and stimulated with 200 ng/mL PMA and 300 ng/mL Ionomycin for 30 min at 37 °C. Jurkat T-cells (3x10^7 per sample) were washed with ice-cold PBS (-/-) and lysed in 900 µL CoIP buffer (25 mM HEPES (pH 7.5), 150 mM NaCl, 0.2% NP-40, 10% glycerol, 1 mM DTT, 10 mM NaF, 8 mM β-glycerophosphate, 300 µM sodium vanadate) without protease inhibitors for 20 min at 4 °C. After centrifugation (20000 x g, 15 min), 60 µL Strep-Tactin® Sepharose® beads (IBA Life Sciences) were added and the lysate was rotated overnight at 4 °C. Beads were washed 3 times with cold CoIP buffer, suspended in 20 µL CoIP buffer with 3 µM of the respective probe and incubated for 3 hours at 29 °C. The suspension was mixed with 4x SDS-loading buffer and boiled at 95 °C for 5 min. After separation by SDS-PAGE, ABP labeling was assessed by an Amersham Tyhoon 5 Biomolecular Imager (GE Healthcare) (Cy2 channel, laser 488nm/filter 525BP20). MALT1 expression and CYLD cleavage was determined by Western Blot using anti-MALT1 (B-12), anti-CYLD (E-10), and anti-β-Actin (C4) antibodies (all Santa Cruz).

MALT1 ABP labeling in Jurkat T-cell lysate. Jurkat T-cells (3x10^7) were stimulated with 200 ng/mL PMA and 300 ng/mL Ionomycin for 30 min at 37 °C. Inhibitors (S)-Mepazine (25µM), z-VRPR-FMK (25µM, Enzo Life Sciences), and CA-074Me (3µM, Calbiochem) were added to cells for 2 hours prior to stimulation. After stimulation, the cells were washed 3 times with ice-cold PBS (-/-) and lysed in 90 µL CoIP buffer for 20 min at 4 °C. After centrifugation (20000 x g, 15 min), the lysate was incubated with 3 µM of the respective probe for 3 hours at 29 °C. The lysate was mixed with 4x SDS-loading buffer and boiled at 95 °C for 5 min. After separation by SDS-PAGE, ABP labeling was assessed by an Amersham Tyhoon 5 Biomolecular Imager (GE Healthcare) (Cy2 channel, laser 488nm/filter 525BP20).

Cellular MALT1 inhibition. HBL1 cells (grown in standard RPMI medium with 15% FCS) were treated with probes for 5 hours and proteasome inhibitor MG132 (10 µM) was added during the last hour to stabilize RelB cleavage product. Cell were lysed in CoIP buffer (see above) and analyzed by Western blot using anti-RelB (C1E4) and anti-GAPDH (14C10) (all CST).

MALT1 ABP labeling of intact Jurkat T-cells. Parental Jurkat T-cells (1.5x10^7) were incubated in 1 mL RPMI medium containing 3 µM of the respective probe for 3 hours at 37 °C. After incubation, cells were stimulated with 200 ng/mL PMA and 300 ng/mL Ionomycin for 30 min at 37 °C. The cells were centrifuged for 4 min at 350 x g at 4 °C, and washed three times with ice-cold PBS (-/-). The cells were lysed in 120 µL CoIP buffer for 20 min at 4 °C, and centrifuged at 20.000 x g for 15 min. The supernatant was mixed with 4x SDS-loading buffer and boiled at 95 °C for 5 min. After separation by SDS-PAGE, ABP labeling was assessed by an Amersham Tyhoon 5 Biomolecular Imager (GE Healthcare) (Cy2 channel, laser 488nm/filter 525BP20).

ASSOCIATED CONTENT

Supporting Information. Supplemental Figures S1-S7 and HPLC purity data

AUTHOR INFORMATION

Corresponding Author

*E-mail: steven.verhelst@kuleuven.be; steven.verhelst@isas.de; +32 16 374517.

Funding Sources

We acknowledge financial support from Research Foundation Flanders FWO (project number GoD8617N), the Ministerium für Kultur und Wissenschaft des Landes Nordrhein-Westfalen, the Regierende Bürgermeister von Berlin–inkl. Wissenschaft und Forschung, and the Bundesministerium für Bildung und Forschung. DK was supported by funding from the Deutsche Forschungsgemeinschaft (SFB 1054 project A04) and BT by a grant from Slovene Research Agency (P1-0140). High resolution mass spectrometry was made possible by the support of the Hercules Foundation of the Flemish Government (grant 20100225–7).

Notes

The authors declare no competing financial interests.

ACKNOWLEDGMENT

We thank Jan Pascal Kahler for synthesis of the BODIPY fluorophore and Karel van de Plassche for help with the *in silico* docking procedure.

ABBREVIATIONS

ABP, activity-based probe; ACC, 7-Amino-4-carbamoylmethylcoumarin; AOMK, acyloxymethylketone; BODIPY, boron-dipyrromethene; CatB, cathepsin B; CBM, CARMA1-BCL10-MALT1; DLBCL, diffuse large B cell lymphoma; HyCoSuL , hybrid combinatorial substrate library; JNK, Jun N-terminal kinase; MALT1, mucosa-associated lymphoid tissue lymphoma translocation protein 1; MS, Multiple Sclerosis; NF-κB, nuclear factor κB; NHL, non-Hodgkin lymphoma; Pbf, 2,2,4,6,7-pentamethyldihydrobenzofuran-5-sulfonyl.

REFERENCES

(1) Juilland, M.; Thome, M. Holding All the CARDs : How MALT1 Controls CARMA / CARD-Dependent Signaling. *Front. Immunol.* **2018**, *9*, 1927.

(2) Meininger, I.; Krappmann, D. Lymphocyte Signaling and Activation by the CARMA1-BCL10-MALT1 Signalosome. *Biol. Chem.* **2016**, *397* (12), 1315–1333.

(3) Fontán, L.; Gray, N. S.; Melnick, A.; Fontán, L.; Qiao, Q.; Hatcher, J. M.; Casalena, G.; Us, I.; Teater, M.; Durant, M.; Du, G.; Xia, M.; Bilchuk, N.; Chennamadhavuni, S.; Palladino, G.; Inghirami, G.; Philippar, U.; Wu, H.; Scott, D. A.; Gray, N. S.; Melnick, A. Specific Covalent Inhibition of MALT1 Paracaspase Suppresses B Cell Lymphoma Growth

Graphical Abstract Find the Latest Version : Specific Covalent Inhibition of MALT1 Paracaspase Suppresses B Cell Lymphoma Growth. *J. Clin. Invest.* **2018**, *128* (10), 4397–4412.

(4) Ruland, J.; Hartjes, L. CARD–BCL-10–MALT1 Signalling in Protective and Pathological Immunity. *Nat. Rev. Immunol.* **2019**, *19* (2), 118–134.

(5) Fontán, L.; Qiao, Q.; Hatcher, J. M.; Casalena, G.; Us, I.; Teater, M.; Durant, M.; Du, G.; Xia, M.; Bilchuk, N.; Chennamadhavuni, S.; Palladino, G.; Inghirami, G.; Philippar, U.; Wu, H.; Scott, D. A.; Gray, N. S.; Melnick, A. Specific Covalent Inhibition of MALT1 Paracaspase Suppresses B Cell Lymphoma Growth. *J. Clin. Invest.* **2018**, *128* (10), 4397–4412.

(6) Nagel, D.; Spranger, S.; Vincendeau, M.; Grau, M.; Raffegerst, S.; Kloo, B.; Lenz, P.; Hlahla, D.; Neuenschwander, M.; Kries, J. P. Von; Hadian, K.; Do, B.; Lenz, G.; Schendel, D. J.; Krappmann, D. Pharmacologic Inhibition of MALT1 Protease by Phenothiazines as a Therapeutic Approach for the Treatment of Aggressive ABC-DLBCL. *Cancer Cell* **2012**, *22*, 825–837.

(7) Schlauderer, F.; Lammens, K.; Nagel, D.; Vincendeau, M.; Eitelhuber, A. C.; Verhelst, S. H. L.; Kling, D.; Chrusciel, A.; Ruland, J.; Krappmann, D.; Hopfner, K. P. Structural Analysis of Phenothiazine Derivatives as Allosteric Inhibitors of the MALT1 Paracaspase. *Angew. Chemie - Int. Ed.* **2013**, *52* (39), 10384–10387.

(8) Mc Guire, C.; Elton, L.; Wieghofer, P.; Staal, J.; Voet, S.; Demeyer, A.; Nagel, D.; Krappmann, D.; Prinz, M.; Beyaert, R.; van Loo, G. Pharmacological Inhibition of MALT1 Protease Activity Protects Mice in a Mouse Model of Multiple Sclerosis. *J. Neuroinflammation* **2014**, *11* (1), 124.

(9) Jaworski, M.; Marsland, B. J.; Gehrig, J.; Held, W.; Favre, S.; Luther, S. A.; Perroud, M.; Golshayan, D.; Gaide, O.; Thome, M. Malt1 Protease Inactivation Efficiently Dampens Immune Responses but Causes Spontaneous Autoimmunity. *EMBO J.* **2014**, *33* (23), 2765–2781.

(10) Chakrabarty, S.; Kahler, J. P.; van de Plassche, M. A. T.; Vanhoutte, R.; Verhelst, S. H. L. Recent Advances in Activity-Based Protein Profiling of Proteases. In *Activity-Based Protein Profiling*; Cravatt, B. F., Hsu, K.-L., Weerapana, E., Eds.; Springer International Publishing: Cham, 2019; pp 253–281.

(11) Vizovišek, M.; Vidmar, R.; Drag, M.; Fonović, M.; Salvesen, G. S.; Turk, B. Protease Specificity: Towards In Vivo Imaging Applications and Biomarker Discovery. *Trends in Biochemical Sciences*. 2018.

(12) Rebeaud, F.; Hailfinger, S.; Posevitz-fejfar, A.; Tapernoux, M.; Moser, R.; Rueda, D.; Gaide, O.; Iancu, E. M.; Rufer, N.; Fasel, N.; Thome, M. The Proteolytic Activity of the Paracaspase MALT1 Is Key in T Cell Activation. *Nat. Immunol.* **2008**, *9* (3), 272–281.

(13) Eitelhuber, A. C.; Vosyka, O.; Nagel, D.; Bognar, M.; Lenze, D.; Lammens, K.; Schlauderer, F.; Hlahla, D.; Hopfner, K. P.; Lenz, G.; Hummel, M.; Verhelst, S. H. L.; Krappmann, D. Activity-Based Probes for Detection of Active MALT1 Paracaspase in Immune Cells and Lymphomas. *Chem. Biol.* **2015**, *22* (1), 129–138.

(14) Hachmann, J.; Edgington-Mitchell, L. E.; Poreba, M.; Sanman, L. E.; Drag, M.; Bogyo, M.; Salvesen, G. S. Probes to Monitor Activity of the Paracaspase MALT1. *Chem. Biol.* **2015**, *22* (1), 139–147.

(15) Cotrin, S. S.; Puzer, L.; De Souza Judice, W. A.; Juliano, L.; Carmona, A. K.; Juliano, M. A. Positional-Scanning Combinatorial Libraries of Fluorescence Resonance Energy Transfer Peptides to Define Substrate Specificity of Carboxydipeptidases: Assays with Human Cathepsin B. *Anal. Biochem.* **2004**, *335* (2), 244–252.

(16) Poreba, M.; Salvesen, G. S.; Drag, M. Synthesis of a HyCoSuL Peptide Substrate Library to Dissect Protease Substrate Specificity. *Nat. Protoc.* **2017**, *12* (10), 2189–2214.

(17) Schechter, I.; Berger, A. On the Size of the Active Site in Proteases. I. Papain. *Biochem. Biophys. Res. Commun.* **1967**, *27* (2), 157–162.

(18) Hachmann, J.; Snipas, S. J.; van Raam, B. J.; Cancino, E. M.; Houlihan, E. J.; Poreba, M.; Kasperkiewicz, P.; Drag, M.; Salvesen, G. S. Mechanism and Specificity of the Human Paracaspase MALT1. *Biochem. J.* **2012**, *443* (1), 287–295.

(19) Kasperkiewicz, P.; Sonia, K.; Janiszewski, T.; Groborz, K.; Poręba, M.; Snipas, S. J.; Salvesen, G. S.; Drąg, M. Determination of Extended Substrate Specificity of the MALT1 as a Strategy for the Design of Potent Substrates and Activity- Based Probes. *Sci. Rep.* **2018**, *15998* (8), 1–10.

(20) Kato, D.; Boatright, K. M.; Berger, A. B.; Nazif, T.; Blum, G.; Ryan, C.; Chehade, K. A.; Salvesen, G. S.; Bogyo, M. Activity-Based Probes That Target Diverse Cysteine Protease Families. *Nat Chem Biol* **2005**, *1* (1), 33–38.

(21) Vanhoutte, R.; Kahler, P.; Martin, S.; Veen, S. Van. Clickable Polyamine Derivatives as Chemical Probes for the Polyamine Transport System. *ChemBioChem* **2018**, *19*, 907–911.

(22) Bianco, G.; Forli, S.; Goodsell, D. S.; Olson, A. J. Covalent Docking Using Autodock: Two-Point Attractor and Flexible Side Chain Methods. *Protein Sci.* **2016**, *25* (1), 295–301.

(23) Meininger, I.; Griesbach, R. A.; Hu, D.; Gehring, T.; Seeholzer, T.; Bertossi, A.; Kranich, J.; Oeckinghaus, A.; Eitelhuber, A. C.; Greczmiel, U.; Gewies, A.; Schmidt-Supprian, M.; Ruland, J.; Brocker, T.; Heissmeyer, V.; Heyd, F.; Krappmann, D. Alternative Splicing of MALT1 Controls Signalling and Activation of CD4(+) T Cells. *Nat. Commun.* **2016**, *7*, 11292.

(24) Maly, D. J.; Leonetti, F.; Backes, B. J.; Dauber, D. S.; Harris, J. L.; Craik, C. S.; Ellman, J. A. Expedient Solid-Phase Synthesis of Fluorogenic Protease Substrates Using the 7-Amino-4-Carbamoylmethylcoumarin (ACC) Fluorophore. *J Org Chem* **2002**, *67* (3), 910–915.

(25) Rozman, J.; Stojan, J.; Kuhelj, R.; Turk, V.; Turk, B. Autocatalytic Processing of Recombinant Human Procathepsin B Is a Bimolecular Process. *FEBS Lett.* **1999**.

(26) Hassan Hassan Abdellatif, F.; Babin, J.; Arnal-Herault, C.; Nouvel, C.; Six, J. L.; Jonquieres, A. Bio-Based Membranes for Ethyl Tert-Butyl Ether (ETBE) Bio-Fuel Purification by Pervaporation. *J. Memb. Sci.* **2017**, *524*, 449–459.

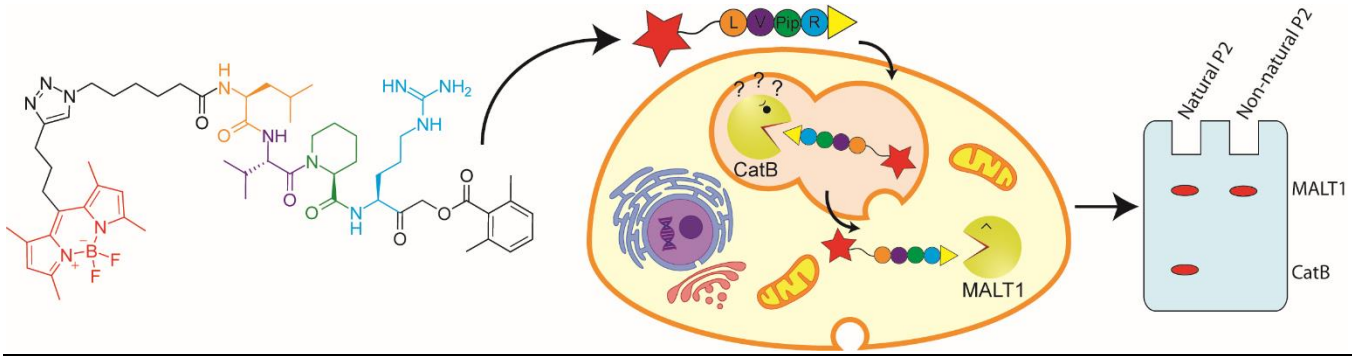
L
V
Pip
R
CatB
MALT1
Natural P2
Non-natural P2
MALT1
CatB